LLNL-JRNL-2010459

Lawrence Livermore National Laboratory

Ion Transport in Self-Assembled Peptoid Membranes with Carbon Nanotube Porin Channels

P CHakma, E Mondarte, M Saraswat, A Noy, C CHen, S ZHang

January 2026

Nano Letters

Disclaimer

This work performed under the auspices of the U.S. Department of Energy by Lawrence Livermore National Laboratory under Contract DE-AC52-07NA27344.

Ion transport in self-assembled peptoid membranes with carbon nanotube porin channels

Mohit Saraswat,[1,2,†] Progyateg Chakma,[3,†,‡] Shuai Zhang,[3,5] Evan Angelo Mondarte,[3] Chun-Long Chen,[3,4,*] and Aleksandr Noy[1,2,*]

[1]Materials Science Division, Physical and Life Sciences Directorate, Lawrence Livermore National Laboratory, Livermore, CA 94550, USA

[2]School of Natural Sciences, University of California Merced, Merced, CA 96343, USA

[3]Physical Sciences Division, Pacific Northwest National Laboratory, Richland, WA 99352, USA

[4]Department of Chemical Engineering, University of Washington, Seattle, WA 98195, USA

[5]Department of Materials Science and Engineering, University of Washington, Seattle, WA 98105, USA

[†]Equal contribution

[‡]Current address: Kennesaw State University, Kennesaw, GA 30144, USA

[*]Correspondence to: CC:*chunlong.chen@pnnl.gov*; AN: *noy1@llnl.gov*

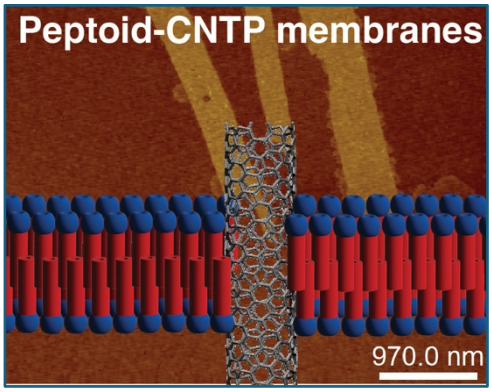

ABSTRACT: Artificial membranes that combine high ionic selectivity with mechanical robustness remain a key challenge for next-generation separation technologies. Here, we report ion transport measurements in biomimetic membranes composed of crystalline peptoid nanosheets co-assembled with carbon nanotube porins (CNTPs). Pure peptoid sheets formed defect-free, ion-impermeable membranes, which were then suspended over small SiN_x nanopore apertures for ion transport measurements. Incorporation of CNTPs into the peptoid sheet matrix made these membranes ion permeable, with ion conductance values consistent with ion transport through individual and multiple carbon nanotube channels. The modularity and molecular order of peptoid membranes, combined with the exceptional conductance properties of CNTPs, position this platform as a versatile framework for assembling programmable, selective, and robust nanofluidic membranes that can bridge the performance gap between biological and synthetic membrane materials.

KEYWORDS: *Biomimetic Membranes; Carbon Nanotube Porins; Peptoid Membranes; Programmable Self-Assembly; Ion Transport.*

Membrane-based separations are essential to modern society, enabling critical processes in water purification,[1] food production[2], and the chemical and pharmaceutical industries.[3-5] While polymer-based membranes dominate these applications due to their versatility, durability, and low cost, their performance still falls short of biological membranes, particularly those incorporating specialized protein pores,[6] ion channels, and ion pumps.[7]

Several key limitations of the polymer membrane platform are responsible for this disparity. Unlike biological membranes, which feature precisely defined, size-selective pores, polymer

membranes exhibit randomly distributed, polydisperse pore structures, making it challenging to achieve the ideal isoporous architecture that can be beneficial for high selectivity and throughput.[8] Polymer membranes rely solely on the polymera single component the polymer itself to form both the pores and the supporting matrix, often forcing compromises that limit overall performance. Finally, biological membranes often have intrinsic self-healing capabilities that allow them to create thin, highly permeable structures that are still robust enough to enable useful function.[9]

To bridge this performance gap, researchers have turned to biomimetic membrane designs that mimic the biological paradigm by incorporating highly selective artificial channels into synthetic matrices.[10, 11] Among the most promising of these channels are carbon nanotube porins (CNTPs), which function as artificial analogues of membrane ion channels. Researchers have used simulations and experimental transport measurements to demonstrate that their hydrophobic, atomically smooth interior pore walls enable ultra-fast water transport,[12] unique ion transport mechanisms,[13] and strong molecular selectivity.[14]

However, the fragility of lipid bilayers has posed a major barrier to the practical application of CNTPs in membrane research. To overcome this problem, our prior work introduced self-assembled peptoid sheet membranes as a robust alternative to the lipid. Peptoids are sequence-defined peptidomimetic polymers capable of self-assembling into crystalline matrix.[15-19] Peptoids, two-dimensional nanosheets that are thermally and chemically stable have excellent. Their durability, modularity, ability to mimic the structural order and complexity of biological systems,[17, 18] and self-repair capabilities[18, 19] make them ideal matrix material for embedding functional nanopores such as CNTPs.[20]

Our earlier work demonstrated that CNTPs can co-assemble with peptoids into stable 2D nanosheets without disrupting the membrane's crystallinity or monomer packing.[15] This co-assembly was verified with molecular dynamics (MD) simulations, Raman spectroscopy, X-ray diffraction (XRD), and atomic force microscopy (AFM) imaging. Additionally, MD simulations showed that the embedded CNTPs remained water-filled, suggesting potential for selective water and ion transport.[15]

In this report, we build upon this foundation to evaluate the ion transport properties of these self-assembled CNTP–peptoid membranes. We report a series of transport experiments that assess the efficiency of ion transport in peptoid membranes with and without CNTPs. Our results revealed that while the self-assembled peptoid membranes were intrinsically impermeable to ions, the incorporation of CNTPs enabled significant ion transport, consistent with ion conductance through carbon nanotubes.[12, 21] These findings not only validate the functional integration of CNTPs into peptoid matrices but also highlight their potential as programmable, durable platforms for advanced separation technologies. By combining the selective transport characteristics of CNTPs with the robustness of peptoid nanosheets, this work opens new avenues for the design of artificial membranes and nanoporous materials with precise, tunable control over solute transport.

The peptoid sequence (*Nbrpe)6(Nhis)(Npm)(Nhis)*, which we chose for this study (Fig. 1a), self-assembles into large micron-sized bilayer sheets.[15, 22] Crucially, our prior work showed that these

sheets can co-assemble with CNTPs without causing significant disruption to the peptoid packing and the resulting membrane integrity. For this work, we have followed the same co-assembly protocol to synthesize both the pure peptoid sheets and peptoid sheets with CNTPs (–Peptoid-CNTP). However, unlike the previous work, which used large 1.5 nm inner diameter CNTPs,[15] for this work we chose to use smaller, 0.8 nm diameter CNTPs, which should offer an even tighter fit into the peptoid sheet structure. These CNTPs also provide well-defined and almost exclusively cation-selective ion conductance of ca. 70 pS per individual nanotube channel.[12] To enable the ion transport measurements, we drop-casted peptoid sheets (Fig. 1b) onto custom supports that consisted of microfabricated SiNx windows with a single ca. 75 nm diameter aperture in the center of the window (see also Suppl. 1 for details of the support).

Assembled pure peptoid sheets showed uniform morphology that was consistent with the previous reports. Significantly, AFM imaging (Fig. 1c) showed that the surface of these sheets was uniform and smooth and largely devoid of any defects. The thickness of the sheets determined by AFM was also similar to the height of other sheets assembled from Nbrpe6[22] (Fig. 1e). In contrast, the surface of the peptoid-CNTP sheets showed distinct protrusions from the sheet surfaces by several nanometers, (Fig. 1d-f) which were consistent with the previously reported morphology of the co-assembled peptoid-CNTP sheets.[15] In addition, we used AFM-based nanomechanical mapping to measure the modulus of the peptoid-CNTP sheets (Suppl. Fig. S2) on mica. The result showed that the CNTP protrusions on the peptoid sheet surface also have a higher elastic modulus than the peptoid sheets. These observations agree with our previous report of the co-assembled peptoid-CNTP that the CNTs co-assembled in the peptoid-CNTP nanosheets show stronger mechanical properties and high elastic moduli.[15] Therefore, the AFM morphology characterization and nanomechanical measurement confirm the co-assembly of CNTPs into peptoid sheets.

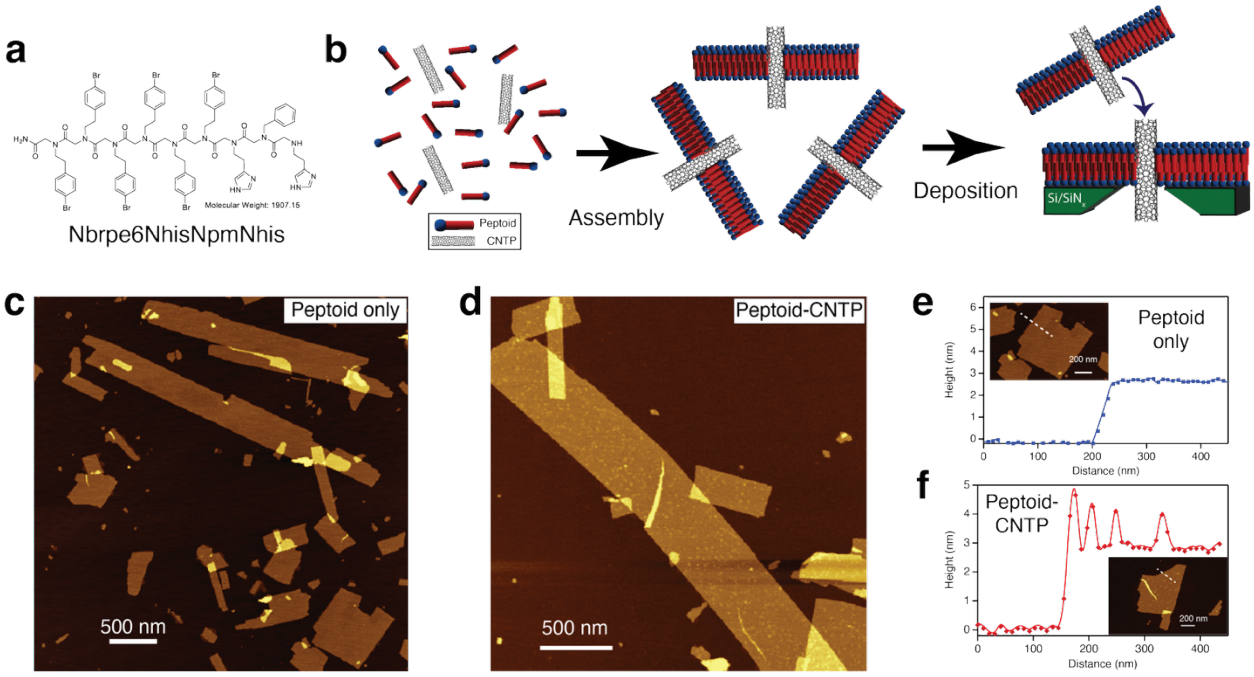

Figure 1. **Assembly and structure of the Peptoid-CNTP membranes**. **a**. Structure of the peptoid used to form the membrane sheets. **b**. Schematics of the assembly protocol used to co-assemble Peptoid-CNTP sheets and deposit them onto the SiN_x aperture. **c,d**. AFM images of the pure peptoid (*c*) and Peptoid-CNTP (*d*) nanosheets. **e,f**. Height profiles for pure peptoid (*e*) and peptoid-CNTP (*f*) nanosheets corresponding to the dashed lines on the inset AFM images.

Proper alignment of the drop-casted peptoid sheet with the SiN_x aperture was critical for the success of our measurements, therefore, before performing ion current measurements we always used AFM imaging to ensure that the aperture was fully covered with the intact peptoid sheet. For the transport measurements, after depositing the peptoid sheets we have mounted the chips into a custom-built fluid cell that sealed the chip between two compartments filled with buffered 1 M KCl solution and used electrodes incorporated into those compartments to record the current-vs-voltage response of the chip with a sensitive current amplifier (Fig. 2a).

Control experiments, where we measured the ion conductance of the open aperture (Fig. 2b) showed very large conductance of 400 nS, which was consistent with ion conductance expected from a 75 nm opening in a SiN_x membrane. When we used this setup to characterize the conductance of pure peptoid membranes, we could not detect conductance beyond the detection limit of our system (~0.2 pS). This result indicates that crystalline nanosheets assembled from pure peptoid (Nbrpe)6(Nhis)(Npm)(Nhis) are virtually ion-impermeable and could be suitable for serving as a robust and programmable matrix to replace lipid bilayers for the insertion of biomimetic artificial channels.[11] Impermeable 2D sheets could also be useful for applications such as anticorrosive coatings.[23] This performance is no surprising given the strongly crystalline nature of these sheets and tight packing of the peptoid monomers. Significantly, this result also points to a good adhesion of the sheets to the chip surface that prevented any significant ion current leaks in our experiments.

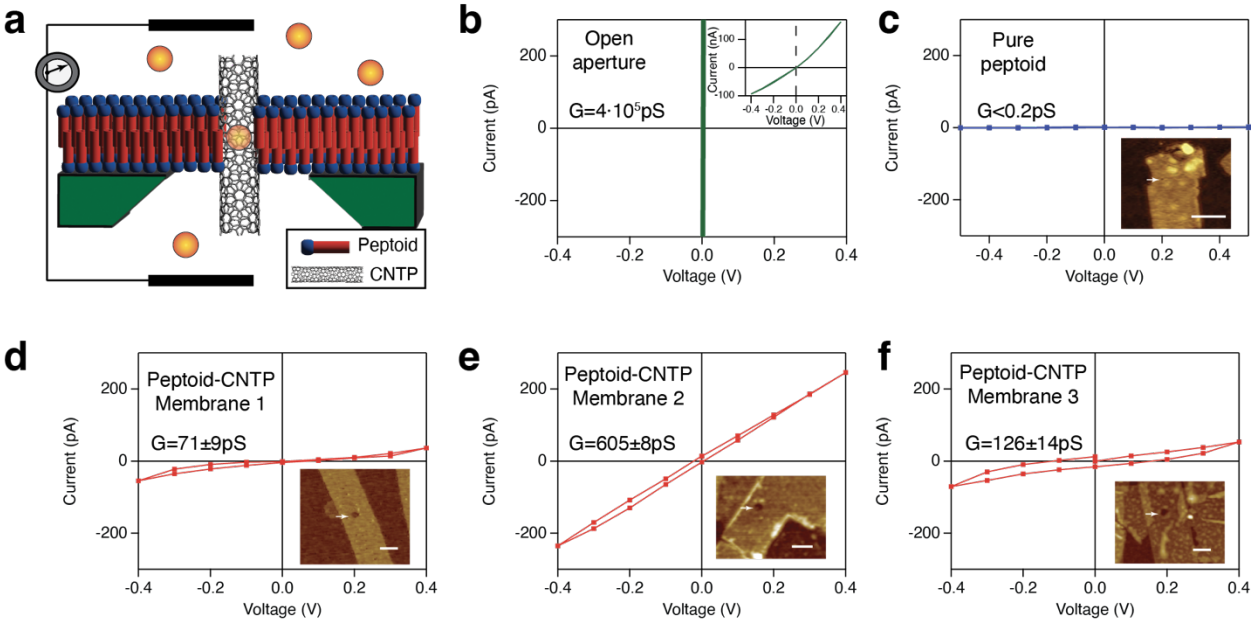

Figure 2. **Ion conductance in Peptoid-CNTP membranes. a**. Schematics of the ion conductance measurement. **b-f**. Current vs. voltage curves recorded for open SiN_x aperture (*b*), pure peptoid sheet (*c*), and peptoid-CNTP sheets (*d-f*). Insets show AFM images of the sample with the white arrows indicating the position of the aperture in the SiN_x support. Scale bar: 200 nm. See Suppl. Fig. S3 for full-scale AFM images of membranes in panels *d-e*.

We then measured ion conductance of the co-assembled Peptoid-CNTP sheets covering a SiN_x aperture. In contrast to the pure peptoid sheet data, these sheets showed strong evidence of ion conductance (Fig. 2d-f). The measured conductance characteristics of the peptoid sheets were consistent over several consecutive measurements, indicating that the sheets were stable. The measured conductance values ranged from ca. 70 pS (Fig. 2d), corresponding to a single CNTP channel,[12] to over 600 pS (Fig. 2e), corresponding to 8 or 9 nanotube pores. These variations were not surprising, as they resulted from a combination of a relatively small size of the aperture on the chips that we used for our measurements and the random nature of CNTP incorporation into the peptoid matrix. AFM imaging and nanomechanical mapping (Suppl. Fig. S2) indicate that the CNTP channels are distributed in the peptoid sheets sparsely with the density roughly on the order of 1 CNTP per $2 \cdot 10^4$ nm^2, indicating that $4.42 \cdot 10^4$ nm^2 apertures used for our experiments should on average contain one or two individual CNTPs. Indeed, the conductance values of two of the samples (Fig. 2d,f) conform to this prediction. Another tested membrane (Fig. 2e) shows larger conductance corresponding to approximately 8 CNTPs. While it is possible that this value resulted from fortuitous series of CNTP incorporation events during co-assembly, we also cannot exclude the possibility of incorporation of a bundle of CNTPs into the peptoid sheet. However, we note that we have not observed any strong evidence of such bundles in the AFM images of peptoid-CNTP sheets.

These results indicate that co-assembly of peptoid-based membrane building blocks with CNTPs is a viable route to creating rationally designed artificial membranes. The modular nature of this system opens up the possibility for independent design optimization of both membrane components to tailor these membranes for particular separation tasks. The semi-crystalline nature of the peptoid sheets, coupled with the previously reported self-healing behavior of these assemblies, also points to the high robustness of these composite membranes. Further refinements in the self-assembly protocols, coupled with the targeted chemical modifications of carbon nanotube pore rims to alter their selectivity, would position peptoid-CNTP assemblies as a versatile biomimetic synthetic membrane platform.

Materials and Methods.

Peptoid synthesis. Peptoid (Nbrpe)6(Nhis)(Npm)(Nhis) was synthesized by following a sub-monomer solid phase synthesis methodology described in the previous papers reported by our team.[22] First, (Nbrpe)6 (~0.09 mmol, one equivalent) was synthesized in an Aapptec Apex 396 robotic synthesizer following the auto-synthesis protocol. Here, 4-bromophenyl ethyl amine (Nbrpe) was used as the primary amine. Then, an acylation reaction was performed by introducing 1.6 mL of a 0.6 M chloroacetic acid solution in

dimethylformamide (DMF), followed by 0.30 mL of a 50% (v/v) N,N'-Diisopropylcarbodiimide (DIC)/DMF solution, and then shaking at room temperature for 15 minutes. The resulting resin was washed with 1.5 mL of DMF (three times) and 1.5 mL of dichloromethane (DCM) (three times). Into that resin, a displacement reaction was carried out by adding 2 mL solution of 0.6 M 2-(4-Imidazolyl)ethylamine (NHis) in N-Methyl-2-pyrrolidone (NMP). The reaction was left shaking for one hour at 40 °C. Finally, the resin was washed with DMF (5 times) and DCM (3 times) to obtain (Nbrpe)6Nhis. Then, one Npm unit was added by a standard manual synthesis acylation step using bromoacetic acid/DIC, followed by a displacement reaction with 0.6 M benzyl amine (Npm) in NMP. Finally, another Nhis unit was added by following the acylation and displacement steps involving the His group described above. The subsequent resin was washed with DMF (5 times) and DCM (3 times), then purified by a Waters 1525 system equipped with an XBridgeTM Prep C18 OBDTM column (10 μm, 19mm× 100mm), and purity verified by Waters ACQUITY reverse phase ultra-pure liquid chromatography UPLC (a gradient of acetonitrile ranging from 5-95 % at 0.4 mL/min over 7 min at 40 °C with an ACQUITYBEH C18, 1.7 μm, 2.1mm× 50mm column) connected with a Waters SQD2 mass spectrometry system.

Peptoid self-assembly and co-assembly with CNTP. Peptoid self-assembly was performed by dissolving 1 μmol of lyophilized peptoid in a 200 μl mixture of acetonitrile and water (1:1 by volume) to produce a 5.0 mM clear solution. This solution was then allowed to undergo slow evaporation for self-assembly. After a few days, gel-like materials containing crystalline nanomaterials were obtained.
Co-assembly of the peptoid with CNTP was carried out following the procedure reported previously.[15] Lyophilized peptoid was dissolved in 100 μl acetonitrile to make a 10.0 mM solution. The solution was sonicated in a sonic bath, if necessary, to obtain a clear solution. Into this clear solution, 200 μL of CNTP aqueous solution was added and mixed until a clear solution was obtained. This resulting solution was allowed to undergo slow evaporation for co-assembly. After a week, gel-like materials containing crystalline nanomaterials were obtained.

Deposition and AFM characterization. AFM imaging was performed using a MultiMode VIII AFM (Bruker, CA) in tapping mode with Multi 75AI-G AFM probes (Budget Sensors) in ambient conditions. For the peptoid-only sample, 1.0 μL of self-assembled gel-like materials was added to 400 μL of deionized (DI) water and mixed thoroughly. From this mixture, 40 μL was placed onto a freshly cleaved mica substrate. After 5 minutes of incubation, the excess water was removed and the sample was air-dried, followed by AFM imaging. For the peptoid-CNTP sample, 5 μL of the mixture, consisting of 1.0 μL of co-assembled gel-like materials in 400 μL of deionized (DI) water, was placed onto a SiNx chip. After 5 minutes of incubation, the excess water was removed and the sample was air-dried, followed by AFM imaging. The Nanoscope Analysis and Gwyddion software was used for offline data processing.

Nanomechanical mapping. Nanomechanical mapping was performed using a Cypher-VRS AFM (Asylum Research, CA) in fast-force mapping mode with Multi 75AI-G AFM probes in ambient conditions. The modulus map was calculated using the Hertz model. The Gwyddion software was used for offline data processing.

Ion conductance measurements. After drop-casting peptoid sheet with or without CNTP channels onto the SiN_x support chip, the chip was then sealed between the two compartments of a custom PEEK testing cell so that the nanosheet-covered aperture on the chip separated the cell into cis and trans reservoirs, with nitrile O-rings and PEEK fittings ensuring a leak-tight seal. Both reservoirs were fitted with Ag/AgCl electrodes and filled with 1 M KCl prepared with 18.2 MΩ cm Milli-Q water and filtered through 20 nm Whatman Anotop 25 Plus filters. Ionic currents were recorded under DC voltage sweeps using a Zurich Instruments, MFLI 500 kHz amplifier operated under custom LabVIEW software. Ion conductance values were obtained from linear fits to the I–V curves.

Acknowledgments. This project was supported by the US Department of Energy, Office of Basic Energy Sciences, Division of Materials Science and Engineering under an award SCW1607 at the Lawrence Livermore National Laboratory (LLNL), and an award FWP 65357 at Pacific Northwest National Laboratory (PNNL). Work at the Lawrence Livermore National Laboratory was performed under the auspices of the US Department of Energy under Contract DE-AC52-07NA27344.

References

(1) Shannon, M.; Bohn, P.; Elimelech, M.; Georgiadis, J.; Marinas, B.; Mayes, A. Science and Technology for Water Purification in the Coming Decades. *Nature* **2008**, *452*, 301-310

(2) Charcosset, C. Classical and recent applications of membrane processes in the food industry. *Food Engineering Reviews* **2021**, *13* (2), 322-343.

(3) Lively, R. P.; Sholl, D. S. From water to organics in membrane separations. *Nat. Mater.* **2017**, *16* (3), 276-279.

(4) Sholl, D. S.; Lively, R. P. Seven chemical separations to change the world. *Nature* **2016**, *532* (7600), 435-437. DOI: 10.1038/532435a.

(5) DuChanois, R. M.; Porter, C. J.; Violet, C.; Verduzco, R.; Elimelech, M. Membrane materials for selective ion separations at the water–energy nexus. *Adv. Mater. (Weinheim, Ger.)* **2021**, *33* (38), 2101312.

(6) Zhong, P. S.; Chung, T.-S.; Jeyaseelan, K.; Armugam, A. Aquaporin-embedded biomimetic membranes for nanofiltration. *J. Membr. Sci.* **2012**, *407*, 27-33.

(7) Fyles, T. Synthetic ion channels in bilayer membranes. *Chem. Soc. Rev.* **2007**, *36* (2), 335-347. DOI: 10.1039/b603256g.

(8) Waldman, R. Z.; Gao, F.; Phillip, W. A.; Darling, S. B. Maximizing selectivity: An analysis of isoporous membranes. *J. Membr. Sci.* **2021**, *633*, 119389.

(9) Bagatolli, L. A.; Stock, R. P. Lipids, membranes, colloids and cells: A long view. *Biochimica et Biophysica Acta (BBA)-Biomembranes* **2021**, *1863* (10), 183684.

(10) Shen, Y.-x.; Saboe, P. O.; Sines, I. T.; Erbakan, M.; Kumar, M. Biomimetic membranes: A review. *J. Membr. Sci.* **2014**, *454*, 359-381.

(11) Tu, Y.-M.; Samineni, L.; Ren, T.; Schantz, A. B.; Song, W.; Sharma, S.; Kumar, M. Prospective applications of nanometer-scale pore size biomimetic and bioinspired membranes. *J. Membr. Sci.* **2021**, *620*, 118968. DOI: https://doi.org/10.1016/j.memsci.2020.118968.

(12) Tunuguntla, R.; Henley, R.; Yao, Y.-C.; Pham, T. A.; Wanunu, M.; Noy, A. Enhanced water permeability and tunable ion selectivity in sub-nanometer carbon nanotube porins. *Science* **2017**, *357*, *792–796*.

(13) Li, Z.; Misra, R. P.; Li, Y.; Yao, Y.-C.; Zhao, S.; Zhang, Y.; Chen, Y.; Blankschtein, D.; Noy, A. Breakdown of Nernst-Einstein relation in carbon nanotube porins. *Nat. Nanotechnol.* **2023**, *18*, 177-183. DOI: 10.1038/s41565-022-01276-0.

(14) Li, Z.; Li, Y.; Yao, Y.-C.; Aydin, F.; Zhan, C.; Chen, Y.; Elimelech, M.; Pham, T. A.; Noy, A. Strong differential monovalent anion selectivity in narrow diameter carbon nanotube porins. *ACS Nano* **2020**, *14* (5), 6269-6275.

(15) Zhang, S.; Hettige, J. J.; Li, Y.; Jian, T.; Yang, W.; Yao, Y. C.; Zheng, R.; Lin, Z.; Tao, J.; De Yoreo, J. J.; et al. Co-Assembly of Carbon Nanotube Porins into Biomimetic Peptoid Membranes. *Small* **2023**, *19* (21), 2206810.

(16) Trinh, T. K. H.; Jian, T.; Jin, B.; Nguyen, D.-T.; Zuckermann, R. N.; Chen, C.-L. Designed Metal-Containing Peptoid Membranes as Enzyme Mimetics for Catalytic Organophosphate Degradation. *ACS Appl. Mater. Interfaces* **2023**, *15* (44), 51191-51203. DOI: 10.1021/acsami.3c11816.
(17) Song, Y.; Wang, M.; Akkineni, S.; Yang, W.; Hettige, J. J.; Jin, H.; Liao, Z.; Mu, P.; Yan, F.; Baer, M.; et al. Highly Bright and Photostable Two-Dimensional Nanomaterials Assembled from Sequence-Defined Peptoids. *ACS Mater. Lett.* **2021**, *3* (4), 420-427. DOI: 10.1021/acsmaterialslett.1c00110.
(18) Jin, H.; Jiao, F.; Daily, M. D.; Chen, Y.; Yan, F.; Ding, Y.-H.; Zhang, X.; Robertson, E. J.; Baer, M. D.; Chen, C.-L. Highly stable and self-repairing membrane-mimetic 2D nanomaterials assembled from lipid-like peptoids. *Nat. Commun.* **2016**, *7*, 12252, Article. DOI: 10.1038/ncomms12252.
(19) Jiao, F.; Chen, Y.; Jin, H.; He, P.; Chen, C.-L.; De Yoreo, J. J. Self-repair and patterning of 2D membrane-like peptoid materials. *Adv. Funct. Mater.* 2016, (26), 8960-8967. DOI: 10.1002/adfm.201602365.
~~(20) Zhang, S.; Hettige, J. J.; Li, Y.; Jian, T.; Yang, W.; Yao, Y.-C.; Zheng, R.; Lin, Z.; Tao, J.; De Yoreo, J. J.; et al. Co-Assembly of Carbon Nanotube Porins into Biomimetic Peptoid Membranes. *Small* **2023**, *19* (21), 2206810, https://doi.org/10.1002/smll.202206810. DOI:~~ https://doi.org/10.1002/smll.202206810 (acccessed 2023/07/08).
(21) Li, Y.; Li, Z.; Misra, R. P.; Liang, C.; Gillen, A. J.; Zhao, S.; Abdullah, J.; Laurence, T.; Fagan, J. A.; Aluru, N.; et al. Molecular transport enhancement in pure metallic carbon nanotube porins. *Nat. Mater.* **2024**, *23* (8), 1123-1130.
(22) Chakma, P.; Chen, Y.; Harris, B. S.; Elhady, Y. W.; Zheng, R.; Bowden, M. E.; Shutthanandan, V.; Bard, A. B.; Trinh, T. K. H.; Zheng, X.; et al. Assembled peptoid crystalline nanomaterials as carbonic anhydrase mimics for promoted hydration and sequestration of CO2. *Nature Communications* **2025**, *16* (1), 7348. DOI: 10.1038/s41467-025-62366-w.
(23) Zhang, Y.; Sun, J.; Xiao, X.; Wang, N.; Meng, G.; Gu, L. Graphene-like two-dimensional nanosheets-based anticorrosive coatings: A review. *Journal of Materials Science & Technology* **2022**, *129*, 139-162.

Ion transport in self-assembled peptoid membranes with carbon nanotube porin channels

Mohit Saraswat,[1,2,†] Progyateg Chakma,[3,†,‡] Shuai Zhang,[3,5] Evan Angelo Mondarte,[3] Chun-Long Chen,[3,4,*] and Aleksandr Noy[1,2,*]

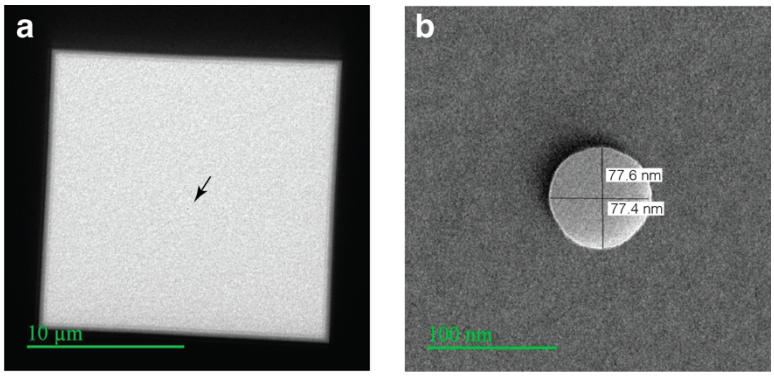

Figure S1. Electron microscopy images of nanopore substrates used for the experiments. **a.** SiN_x support surface. Arrow points to the location of ca.75nm aperture. **b**. Close-up image of the aperture with longitudinal and latitudinal dimensions indicated on the image. *All images courtesy of Norcada, Inc., Edmonton, AB, Canada.*

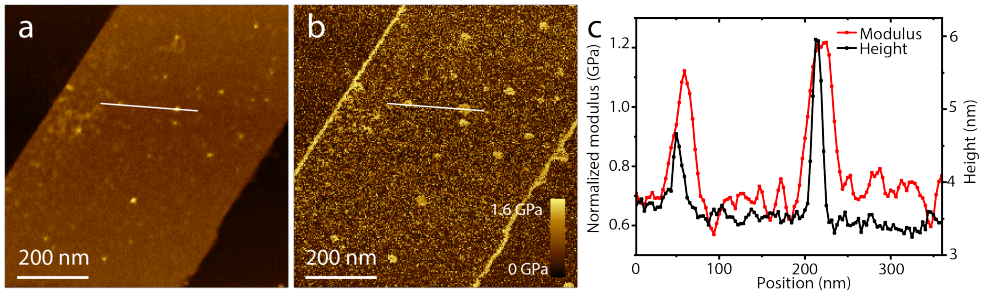

Figure S2. Nanomechanical mapping of peptoid-CNTP. **a, b**. AFM height and the corresponding elastic modulus images of peptoid-CNTP on mica. **c**. Line profiles marked in Panel a and b.

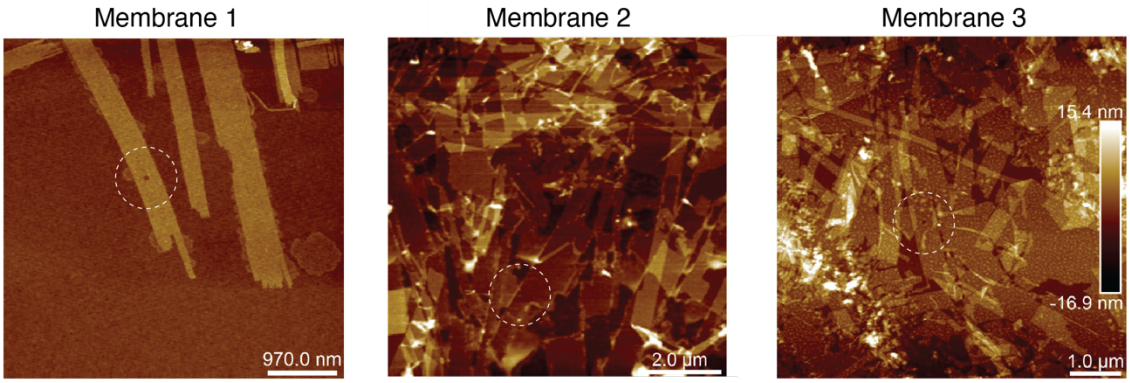

Figure S3. Full-size AFM images of peptoid-CNTP membranes presented on the Figure 2d-f. Dashed line circles indicate the location of the membrane aperture.